PCCP

RSC Publishing

PAPER

trans effect and *trans* influence: importance of metal mediated ligand–ligand repulsion†

Cite this: *Phys. Chem. Chem. Phys.*, 2013, **15**, 17354

Balazs Pinter,*[a] Veronique Van Speybroeck,[b] Michel Waroquier,[b] Paul Geerlings[a] and Frank De Proft*[a]

The *trans* effect and *trans* influence were investigated and rationalized in the aminolysis, a typical nucleophilic substitution reaction, of *trans*-$TPtCl_2NH_3$ complexes (T = NH_3, PH_3, CO and C_2H_4) using energy decomposition analysis, both along the reaction paths and on the stationary points, and Natural Orbital for Chemical Valence analysis. In order to scrutinize the underlying principles and the origin of the kinetic *trans* effect, plausible structural constraints were introduced in the decomposition analysis, which allowed eliminating the distance dependence of the interaction energy components. It was established that the *trans* effect can be rationalized with the interaction of the $TPtCl_2$ and NH_3 fragments in the reactant state and $TPtCl_2$ and $(NH_3)_2$ fragments in the transition state. It was evinced quantitatively that the σ-donor ability of T indeed controls the stability of the reactant, whereas in the case of π-acids, backdonation stabilizes the transition state, for which conceptually two mechanisms are available: intrinsic and induced π-backdonation. In the destabilization of the reactant and also in the labilization of the leaving group (*trans* influence) repulsion plays a more important role than orbital sharing effects, which are the cornerstones of the widely accepted interpretations of the *trans* influence, such as competition for donation or limitation of the donation of the leaving group by the *trans* ligand T. This repulsive interaction was rationalized both in terms of donated electron density and also in the molecular orbital framework. NOCV orbitals indeed clearly show that the σ-*trans* effect can be envisioned as a donation from the *trans* ligand not only to the metal but also to the σ* orbital of the metal-leaving group bond, which manifests as a repulsion between the metal and the leaving group.

Received 7th June 2013,
Accepted 18th August 2013

DOI: 10.1039/c3cp52383g

www.rsc.org/pccp

Introduction

The *trans* effect is a well-known phenomenon in the ligand substitution reaction in square planar and octahedral transition metal complexes.[1,2] It ranks ligands on the basis of their effect on the substitution rate of the leaving group *trans* to their position. In practice, for example, it plays a pivotal role in the mode of action of Pt^{II}-based anticancer drugs[3] (cisplatin, oxaplatin, *etc.*), in the transmetallation steps of various Pd-based catalytic cross-coupling reactions[4] and in the first step of the Shilov reaction,[5] in which alkanes are converted to alcohols using Pt^{II}-based catalysts. For the former, the binding to DNA bases itself is a substitution reaction that is controlled, both regioselectivity and rate, by the *trans* effect.

This ligand effect has been investigated both experimentally[6] and theoretically[7–12] on many occasions. This has resulted in well-established scales to categorize ligands based on their *trans* effect, *i.e.* their overall effect on the rate of ligand substitutions of square planar d^8 complexes.[1b] It was found that good σ-donors, such as PH_3, and good π-acceptors, such as CO, typically accelerate the reaction, whereas *trans* ligands (T) with a poor σ-donor property (*e.g.* H_2O) are less effective in promoting substitution *trans* to themselves. It is a rather dramatic ligand effect spanning several orders of magnitude in rate.[1b] Since it is profoundly an electronic effect, a consensus was reached relatively quickly concerning its mode of action: the σ-donor ability of the *trans* ligand, T, can be linked to the stability of the reactant, whereas π-backdonation to T provides extra stabilization in the trigonal bipyramidal transition state, as depicted in Scheme 1.

The exact mechanism of stabilization–destabilization of the square planar reactant complex by ligand T was the subject of a long debate.[13] It was established that the kinetic *trans* effect

[a] *Eenheid Algemene Chemie (ALGC), Vrije Universiteit Brussel (VUB), Pleinlaan 2, B-1050 Brussels, Belgium. E-mail: Balazs.Pinter@vub.ac.be, fdeprof@vub.ac.be; Fax: +32-2-693-33-17*

[b] *Center for Molecular Modeling, Ghent University, Technologiepark 903, 9052, Zwijnaarde, Belgium*

† Electronic supplementary information (ESI) available: Analysis of the effect of the reference systems and Cartesian coordinates of the optimized structures. See DOI: 10.1039/c3cp52383g

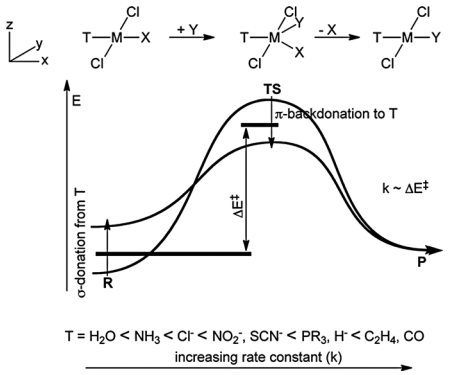

Scheme 1 Proposed mechanisms to influence the activation energy of substitution of X ($\Delta E^{\ddagger}$) with *trans* ligand T.

and *trans* influence, *i.e.* the effect of ligand T on the strength of the metal–ligand bond *trans* to T – manifested for example in the metal–ligand bond distance[9e,14–17] – are related phenomena.[8,13] Early electrostatics based explanations of the latter effect[9d] were revised later to orbital interaction based arguments,[1a,8,9b,e,f,11,13] which formally can be summarized as follows: the *trans* influence and the σ-*trans* effect are caused by "a competition between the ligands to donate their electron density to the central Pt^{II} atom".[11] Accordingly, a good σ-donor labilizes the ligand *trans* to itself by limiting its donation to the metal and *vice versa*.

Most probably the core of this concept originates from the paper of Burdett and Albright[9f] who derived that, in general, the stabilization energy of a bond also depends upon the properties of ligands sharing the orbital involved in the bond. For example for the reactant in Scheme 1, $TMCl_2X$, the σ-bond stabilization of the M–T and M–X bonds was derived to be

$$\Sigma MT(\sigma) = 2\beta_\sigma S_{\sigma T}{}^2 - 2\gamma_\sigma(S_{\sigma T}{}^4 + S_{\sigma T}{}^2 S_{\sigma X}{}^2) \qquad (1a)$$

$$\Sigma MX(\sigma) = 2\beta_\sigma S_{\sigma X}{}^2 - 2\gamma_\sigma(S_{\sigma X}{}^4 + S_{\sigma X}{}^2 S_{\sigma T}{}^2) \qquad (1b)$$

where β_σ and γ_σ are parameters depending on the energies of the interacting orbitals and $S_{\sigma X}$ and $S_{\sigma T}$ are the overlap integrals between the σ-orbital of ligands X and T and the metal d orbital ($d_{x^2-y^2}$), respectively. These expressions simply show that the energy of the M–X bond decreases if the overlap between M and T ($S_{\sigma T}$) increases, that is, if T is a stronger σ-donor. However, note that this term appears only as a secondary effect in eqn (1a) and (1b), serving as a correction factor to the first order term implying that orbital sharing is not a primary factor, which is actually not consistent with the magnitude of the *trans* effect.

The donation-competing ligand argument is, nevertheless, a powerful and widespread concept due to its consistency with the observed experimental, both kinetic and structural, data and with the chemical intuition on the electron donating ability of ligands. In addition, it has received support from various theoretical studies.[8,9e,11,18] The majority of these theoretical studies were carried out on fully optimized structures in which the M–X (*trans* to T, Scheme 1) bond was also let to relax to its equilibrium value. The shortening and lengthening of the M–X bond as a function of T is a clear manifestation of the effect of T,

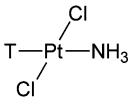

T	d(Pt-NH_3)	P(Pt-NH_3)	P(Pt-T)
H_2O	2.00 Å	0.3370	0.2406
H_2S	2.00 Å	0.3244	0.4295
H^-	2.00 Å	0.3077	0.6069

Scheme 2 Overlap population (P) of Pt–NH_3 and Pt–T as a function of T.[8]

however, comparing structures with different M–X bond lengths might influence the conclusions about the origins of the intrinsic weakening and strengthening of the M–X bond by T. A hint of this problem was given by Zumdahl and Drago, who investigated the overlap population between Pt and the leaving group, NH_3, as a function of T with a *fixed* Pt–NH_3 distance of 2 Å.[8] From this study, Scheme 2 shows the reduced overlap population (P) obtained from Mulliken population analysis for a weak (H_2O), medium (H_2S) and a very strong donor (H^-). As Scheme 2 shows, P(Pt–NH_3) indeed slightly varies with T from 0.34 to 0.32 and to 0.31, respectively; this change is, however, very minor when compared to the overlap integral change for the T–Pt interaction (0.24–0.61). This result rather indicates that the donation of the leaving group is affected only slightly by the donation of T, in line with eqn (1b), but, then again, in contrast to the observed magnitude of the *trans* effect.[1a]

As the oversimplified example in Scheme 2 demonstrates, the recent, widely accepted rationalization of the labilization of the ligand *trans* to T is not complete. In this study, we present a theoretical study using a very powerful tool, energy decomposition analysis, to reveal why a bond elongates if a strong σ-donor binds from the opposite site of the metal, *i.e.* the *trans* influence. The same method was recently applied for this purpose and it was nicely presented that a longer metal–ligand bond is associated with a weaker orbital interaction, as expected.[9e] In this study, we will demonstrate that the latter conclusions are to some degree influenced by the bond length discussion mentioned above. Our results and new concepts are also rationalized within the molecular orbital framework in detail throughout the paper. Our ultimate purpose is to rationalize the phenomenon of the *trans* effect, so we also quantify the effect of back-donation in the transition state and investigate whether or not σ-donation induces extra stabilization in the TS as was proposed by Zumdahl and Drago.[8]

Methodology

We investigated the aminolysis, a typical nucleophilic substitution reaction, of four square planar platinum complexes ($TPtCl_2NH_3$, T = NH_3, PH_3, CO and C_2H_4) differing only in the *trans* ligand T (Fig. 1). The analysed *trans* ligands include two pure σ-donors of different strength (NH_3 and PH_3[19]) and two ligands with π-acceptor properties, *i.e.* π-acids (CO and C_2H_4). Geometry and transition state optimizations and intrinsic reaction coordinate calculations were performed using the M06[20] density-functional coupled with the cc-pVDZ-pp[21] basis set for Pt and the cc-pVDZ basis[22] for light atoms. The energies of the optimized structures were reevaluated using the triple-ζ basis set cc-pVTZ(-pp).[23] Analytical vibrational frequencies within the harmonic approximation were computed with the

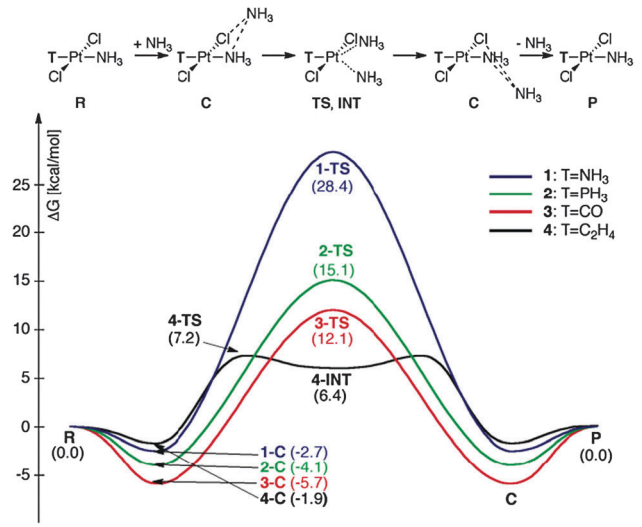

Fig. 1 Investigated systems **1–4** and the corresponding computed reaction profiles (ΔG in kcal mol^{-1} at the M06/cc-pVTZ(-pp)//M06/cc-pVDZ(-pp) level at 298.15 K).

cc-pVDZ(-pp) basis set to confirm minima or saddle points on the potential energy surface. All of these calculations were carried out using Gaussian 09.[24]

High level *ab initio* energy calculations at the CCSD(T)/cc-pVTZ(-pp)[25] level were also carried out on the M06/cc-pVDZ equilibrium structures using MOLPRO[26] to verify the reliability of DFT based techniques in predicting activation energies. Subsequent energy decomposition analysis was performed at the PBE/TZ2P(small core)/ZORA[27,28] level as implemented in ADF2012.[29] Our analysis shows that the energy decomposition analysis is not sensitive to the size of the basis set (Tables S3–S5, ESI†) and that TZ2P reproduces the results of the quadruple-ζ QZ4P basis set within 1 kcal mol^{-1}. The relative stability of stationary points along the reaction paths was also evaluated using the latter method/program package combination.

Within fragment-based approaches, such as the one available in ADF, the potential energy change ΔE can be expressed in terms of the preparation energy ΔE_{prep},[28a,30] which is the energy associated with the geometrical deformation of the fragments from their starting (equilibrium) structure, and the interaction energy between the fragments ΔE_{int} (eqn (2)).

$$\Delta E = \Delta E_{\text{prep}} + \Delta E_{\text{int}} \quad (2)$$

$$\Delta E_{\text{int}} = \Delta E_{\text{Pauli}} + \Delta V_{\text{elstat}} + \Delta E_{\text{oi}} \quad (3)$$

The interaction energy can be further decomposed into three physically meaningful terms (eqn (3)), ΔE_{Pauli}, ΔV_{elstat} and ΔE_{oi}, using the Ziegler–Rauk decomposition scheme.[31] The electrostatic interaction contribution (ΔV_{elstat}) represents the classical Coulomb interaction between the fragments with unperturbed charge distributions. The Pauli repulsion term, ΔE_{Pauli}, embodies the repulsive filled–filled orbital interaction, which is the origin of the steric effect between the reactants.[32] The orbital interaction energy, ΔE_{oi}, calculated in the energy decomposition analysis corresponds to the stabilization caused by the interactions between the occupied molecular orbitals on one fragment and the unoccupied molecular orbitals of the other fragment, as well as by the mixing of occupied and virtual orbitals within the same fragment (intrafragment polarization) upon the formation of the assembled structure from the fragments. The density reorganization which is associated with the latter process and which gives rise to ΔE_{oi} can be expressed in Natural Orbitals for Chemical Valence (NOCV), defined as the eigenvectors that diagonalize the deformation density (eqn (4)),[33]

$$\Delta\rho(r) = \rho - \rho^0 \quad (4)$$

being the difference between the total density ρ of the composed molecule and the sum ρ^0 of the densities of the initial fragments. It is a general property of a subtraction of two idempotent density matrices that eigenvalues appear pairwise, so that the deformation density (eqn (5)) can be expressed as a sum of pairs of complementary eigenfunctions (ψ_k, ψ_{-k}) corresponding to the eigenvalues ν_k and $-\nu_k$:

$$\Delta\rho(r) = \sum_{k=1}^{M/2} \nu_k \left[-\psi_{-k}^2(r) + \psi_k^2(r)\right] = \sum_{k=1}^{M/2} \Delta\rho_k(r) \quad (5)$$

This implies that the eigenvalue ν_k is the number of electrons that is transferred from the orbital ψ_k to $-\psi_k$ upon bond formation. In this study the expression of an NOCV is simply used for the density deformation, $\Delta\rho_i$, represented by a complementary NOCV pair:

$$\Delta\rho_i(r) = \nu_i[-\psi_{-i}^2(r) + \psi_i^2(r)] \quad (6)$$

We performed the energy decomposition analysis along the reaction path in two ways introduced by Bickelhaupt *et al.*[30a,34] and by Frenking *et al.*[35] The main differences in the two approaches are the choice of fragments and the reference point of the reaction path. The former method identifies the two fragments with the two reactants (the Activation Strain Model (ASM)), whereas the latter rather defines the outgoing and incoming substituents, which are directly involved in the bond-breaking/formation process, as one fragment and the remaining core moiety as the other fragment. Considering the reference point, the activation strain model uses the prereactive σ-complex as the zero level, which has the advantage that the analyzed activation barriers are always positive, whereas the relative energies of the species are given with respect to the separated reactants in the method introduced by Frenking *et al.*[35] In the latter case the relative energy of the species along the reaction, which is called the critical energy, can also be negative,[36] but it is independent of the stability of the prereactive σ-complex. In our approach, the reference point is chosen to be the two reactants separated by an infinite distance, whereas we use fragments $TPtCl_2$ and $(NH_3)_2$ along the reaction path. Note that because there is no interaction between the incoming ammonia and the $TPtCl_2$ fragment at an infinite distance, *i.e.* in the reactant state, the interaction energy and its components are determined solely by the interaction of the $TPtCl_2$ and the leaving NH_3 fragments in the

square planar reactant complex $TPtCl_2NH_3$. Our analysis with reactant fragments, *i.e.* $TPtCl_2NH_3$ and NH_3, along the reaction coordinate (Fig. S1–S4, ESI†) as well as an energy decomposition analysis between fragments T and $PtCl_2NH_3$ for reactant states and T and $PtCl_2(NH_3)_2$ for transition states (Table S2, ESI†) can be found in the ESI.†

Results

Table 1 summarizes the calculated activation energies for the investigated aminolysis reactions using various methods. The agreement between M06 and CCSD(T) results is very good; for systems **2–4** the deviation in the activation energy using DFT and *ab initio* methods is less than 1 kcal mol^{-1}, whereas for **1** it is only about 3 kcal mol^{-1}. This result indicates that the M06 functional-based protocol is capable of properly describing the structures as well as the energetics of the investigated systems. In addition, the PBE activation barriers and intermediate stabilities also show very good agreement with the M06 and CCSD(T) values with deviations of only a few kcal mol^{-1}, ensuring the confident use of this protocol in studying the systems in question.

Fig. 1 shows the calculated reaction profiles of the aminolysis with T = NH_3, PH_3, CO and C_2H_4. In the case of T = NH_3, PH_3 and CO, these profiles have the typical characteristics of an interchange (I) type substitution mechanism, *i.e.* starting from the reactant (**R**) the reaction proceeds through a prereactive σ-complex (**C**), a transition state (**TS**) with a symmetric trigonal bipyramidal (tbp) geometry and a subsequent σ-complex (**C**), followed by the product (**P**). The reaction also proceeds through an interchange mechanism for T = C_2H_4, however in this case the symmetric tbp geometry corresponds to an intermediate (**INT**) with similar energy to the **TS**. These findings are consistent with that of former computational mechanistic studies.[11,37] The trend of computed apparent barrier heights, $\Delta G^{\ddagger}_{NH_3} > \Delta G^{\ddagger}_{PH_3} > \Delta G^{\ddagger}_{CO} > \Delta G^{\ddagger}_{C_2H_4}$, is in agreement with the observed *trans* effect strength order of the ligands.[1b,38] Note that the relative energies of the species are given with respect to the separated reactants. Accordingly, we will analyse how T influences the energy difference between the isolated reactants and transition states, which, in line with the terminology of Frenking *et al.*,[35] will be called the critical energy. Nevertheless, intrinsic energy barriers (energies relative to the prereactive complex, **C**) also give the same reactivity order.

Fig. 2 shows the change in the critical energy (ΔE) and its contributors, preparation ($\Delta\Delta E_{prep}$) and interaction energy ($\Delta\Delta E_{int}$) along the IRC, projected to the d(Pt–N2) distance as the reaction coordinate. These graphs start at a d(Pt–N2) distance of 3 Å and end at the trigonal bipyramidal structure, which is the transition state for T = NH_3, PH_3, and CO and the intermediate for C_2H_4. Again, note that all plotted energy values are referred to the reactants at infinite separation. As can be seen from Fig. 2, the energy reaction profile (ΔE) is in agreement with the free energy profile (ΔG) depicted in Fig. 1, still reflecting the *trans* effect exhibited by the four ligands considered. Separation of the critical energy into preparation and interaction energy contributions indicates that our current fragmentation applied indeed results in an almost strain-free

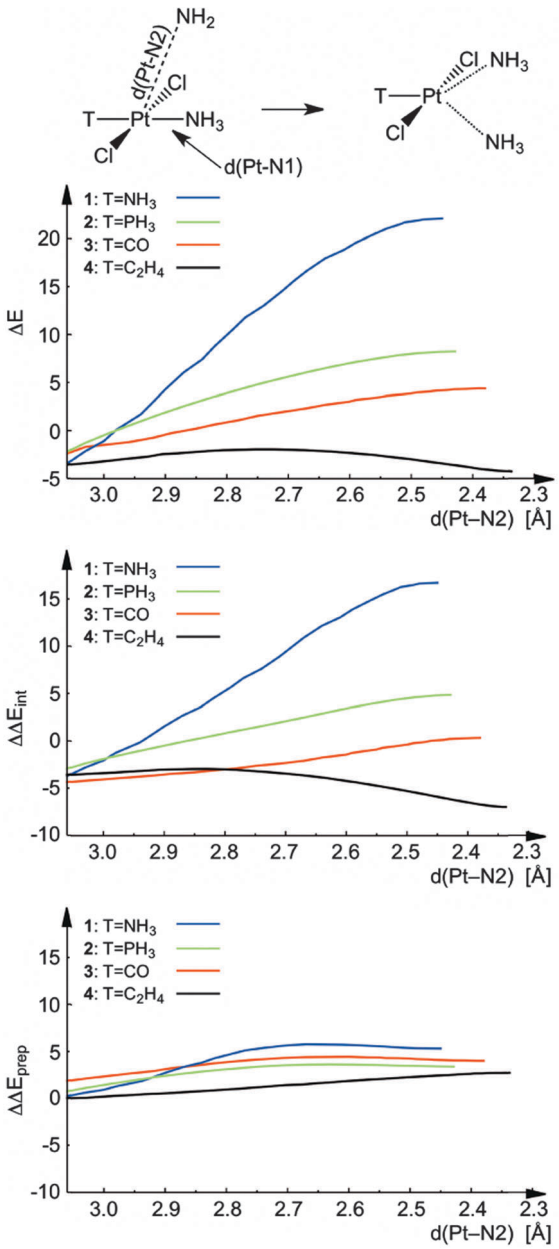

Fig. 2 Critical energy (ΔE) and its contributions, such as interaction energy ($\Delta\Delta E_{int}$) and preparation ($\Delta\Delta E_{prep}$) along the reaction coordinate projected onto the Pt–N2 distance. Energy values are given in kcal mol^{-1}.

Table 1 Calculated energy barriers and free energy barriers using different methods in kcal mol^{-1}. The relative stability of **4-INT** is given in brackets

	$\Delta E^{\ddagger}$				$\Delta G^{\ddagger}$ (298.15 K)
	T	M06	PBE	CCSD(T)	M06
1	NH_3	18.2	22.1	21.4	28.4
2	PH_3	6.4	8.2	7.4	15.1
3	CO	3.2	4.4	3.9	12.1
4	C_2H_4	−4.1	−2.1	−4.7	7.2
		(−4.5)	(−4.3)	(−6.8)	(6.4)

situation, *i.e.* $\Delta E_{prep} \approx 0$, where the total electronic energy is determined dominantly by the interaction energy between the two fragments. Consequently, because the residual strain contribution is very similar for systems **1–4**, the different *trans* effects of the ligands can be scrutinized on pure electronic origins along the interaction of the $TPtCl_2$ and $(NH_3)_2$ fragments with different T.

The energy decomposition in Fig. 3 reveals that $\Delta\Delta E_{int}$ becomes less stabilizing towards the transition state because electrostatic ($\Delta\Delta V_{elstat}$) and orbital interactions ($\Delta\Delta E_{oi}$) become less stabilizing whereas, in contrast, $\Delta\Delta E_{Pauli}$ actually becomes less repulsive. This trend is analogous to that found by Bickelhaupt[34d] and independently by Frenking for model S_N2 reactions.[35a] Also, the same dilemma arises as in the latter studies: why does the Pauli repulsion drop as a fifth ligand enters the coordination sphere? This behaviour of $\Delta\Delta E_{Pauli}$ was critically addressed by Bickelhaupt and Frenking and the same rationalization applies here: the $TPtCl_2NH_3$ responds to the approach of the incoming NH_3 with a geometrical relaxation (mainly with distortion from the planar structure and elongation of the Pt–N1 bond), which helps to relieve the extra Pauli repulsion.

One additional conclusion that can be drawn from these reaction coordinate diagrams is that the Pt–N2 distance, and consequently the Pt–N1 distance as well, differ significantly for the transition states of **1–4**. For example, the transition state is the least compact for T = NH_3 with d(Pt–N2) of 2.45 Å, whereas for T = CO the incoming ammonia has to approach the metal to a distance of 2.38 Å to reach the transition state. One can expect that this distance actually correlates with and represents the stability of the transition state. Surprisingly, however, interaction energies (ΔE_{int}) between $TPtCl_2$ and $(NH_3)_2$ fragments calculated in the equilibrium geometry of the transition states without referencing to the reactant state, listed in Table 2, do not reflect the relative stabilities of the TSs and barrier heights expected on the basis of the *trans* effect strength. For example, there is an activation energy difference of more than 10 kcal mol^{-1} between NH_3 and PH_3, however ΔE_{int} gives very similar interaction energies between $TPtCl_2$ and $(NH_3)_2$ fragments for T = NH_3 and PH_3. This analysis only allows the distinction between pure σ-donor and π-acid type ligands exhibiting interaction energies of about −38 and −49 kcal mol^{-1}, respectively. However, almost no difference emerges between systems of the same class. The components of the interaction energy, however, vary from system to system and overall show that the stronger Pauli repulsion is always accompanied with more stabilizing electrostatic and orbital interactions. Note that this behavior of ΔE_{Pauli}, ΔV_{elstat} and ΔE_{oi} is fully consistent with the observed changes as a function of the Pt–N2 distance as depicted in Fig. 2. As the transition states get more compact Pauli repulsion increases and the electrostatic and orbital interactions become more attractive. This collective behaviour of the energy components is discussed later for the structurally less complex reactant complexes where it is also apparent.

The fact that the interaction energy between $TPtCl_2$ and $(NH_3)_2$ fragments calculated in the transition state cannot account for the energy barrier alone clearly indicates that the stability of the reactant has a prominent effect on the barrier

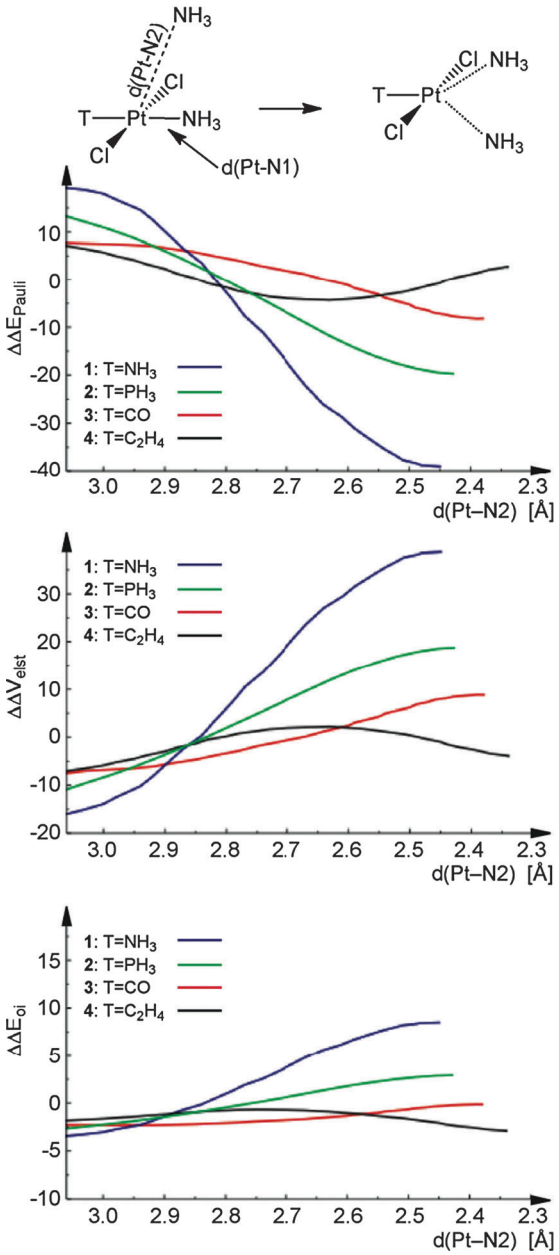

Fig. 3 Components of interaction energy ($\Delta\Delta E_{int}$): Pauli repulsion ($\Delta\Delta E_{Pauli}$), electrostatic interaction ($\Delta\Delta V_{elst}$) and orbital interaction ($\Delta\Delta E_{oi}$) along the reaction coordinates projected onto the Pt–N2 distance. Energy values are given in kcal mol^{-1}.

Table 2 Average of the Pt···NH_3 distances d(Pt–N1) and d(Pt–N2), d(Pt–N), in the transition states (intermediate for **4**) in Å, interaction energy (ΔE_{int}) and its components (ΔE_{Pauli}, ΔV_{elstat} and ΔE_{oi}) in kcal mol^{-1}, calculated between $TPtCl_2$ and $(NH_3)_2$ fragments in the equilibrium transition state structures

	T	d(Pt–N)	ΔE_{Pauli}	ΔV_{elstat}	ΔE_{oi}	ΔE_{int}
1-TS	NH_3	2.448	89.1	−83.9	−43.9	−38.6
2-TS	PH_3	2.428	100.1	−90.4	−46.8	−37.1
3-TS	CO	2.375	118.1	−107.6	−59.6	−49.1
4-INT	C_2H_4	2.325	128.8	−117.3	−61.4	−49.8

height and consequently is an important quantity in determining the *trans* effect. A clear manifestation of the effect of T on $TPtCl_2NH_3$ is the elongation of the Pt–N bond *trans* to T, which is the *trans* influence. It is proposed frequently that the elongation of the bond *trans* to T also comes with the overall destabilization of the complex, *i.e. trans* influence represents not only a geometrical distortion caused by T but also its stabilization–destabilization effect. Recently, Ziegler and co-workers carried out an energy decomposition analysis on $TNiCl_2NH_3$ complexes and indeed found that the longer the Ni–NH_3 bond *trans* to T, the weaker the metal–NH_3 interaction.[9e] Thus, in order to completely understand the factors by which T determines the barrier height, we have to analyze how T influences the stability of the reactant.

Pt–N1 bond lengths calculated for $TPtCl_2NH_3$ complexes (T = NH_3, PH_3, CO and C_2H_4), given in Table 3, reflect a *trans* influence strength order of $NH_3 < CO < C_2H_4 \sim PH_3$. Energy decomposition analysis along the Pt–N1 bond indicates (Table 3) that, as expected, the longer the Pt–N1 bond the smaller the interaction energy (ΔE_{int}) between the $TPtCl_2$ and NH_3 fragments. This finding clearly indicates that T indeed plays a significant role in the stabilization/destabilization of the reactant. As Table 3 also shows, all three components equally contribute to the change in ΔE_{int}; the repulsive filled–filled orbital interaction (ΔE_{Pauli}) decreases, whereas the attractive electrostatic (ΔV_{elstat}) and orbital (ΔE_{oi}) interactions become less stabilizing with increasing bond distance, *i.e.* with stronger *trans* influence exhibiting T. It is important to note that the conventional grouping of Pauli repulsion and electrostatic interaction into steric or non-orbital interaction would diminish the effect of these two terms and would exaggerate the importance of orbital interaction. Consequently, weaker orbital interaction was proposed recently to be the origin of the Ni–NH_3 bond elongation in $TNiCl_2NH_3$ complexes when T is a ligand with strong *trans* influence.[9e]

Another less traditional partitioning invokes the combination of ΔE_{Pauli} and ΔE_{oi}, which represents all the interactions coming from orbitals, both occupied and unoccupied ones, between the two fragments. This quantity is also almost constant for all T, misleadingly suggesting that the *trans* influence is actually an electrostatic phenomenon. Instead of such partitioning, one has to realize that the trends observed for all three components critically depend on the Pt–N1 distance. Elongation of a bond diminishes ΔE_{Pauli}, ΔV_{elstat} and ΔE_{oi}, too, just as observed for the Pt–NH_3 interaction in Table 2. Thus, the only apparent trend that can be established from this and similar analyses is the distance dependence of the energy components. Since this trend obscures the subtle differences, which would actually reveal the origin(s) of bond weakening and elongation, one has to get rid of this effect, for example using the following procedure.

To eliminate the distance dependence of the various terms and reveal the origin (and not the manifestation) of the Pt–N1 bond elongation in the reactant, which is referred to as the *trans* influence, we carried out the decomposition analysis at fixed Pt–N1 distances for T = NH_3, PH_3, CO and C_2H_4. Our protocol for creating structures with constant Pt–N1 bond length, but with different T, is illustrated in Scheme 3. Starting from the equilibrium structure of $NH_3PtCl_2NH_3$ we systematically replace the NH_3 *trans* ligand by PH_3, CO and C_2H_4 using the geometries they adopt in $PH_3PtCl_2NH_3$, $COPtCl_2NH_3$, and $C_2H_4PtCl_2NH_3$, respectively. This methodology ensures that the interaction energy between the $TPtCl_2$ and NH_3 fragments is solely determined by the *trans* ligand T.

Table 4 gives the results of the decomposition analysis with constrained Pt–N1 distances for the reactant state. The total interaction energies differ negligibly from the original decomposition analysis (Table 3 *vs.* Table 4), *i.e.* not much error is induced with the geometrical constraint, and it still reflects the observed *trans* influence strength of ligands T, but this analysis now clearly pinpoints Pauli repulsion as the dominant factor in determining the strength of the Pt–N1 bond. The stronger the *trans* influence of the ligand, the higher the contribution of the

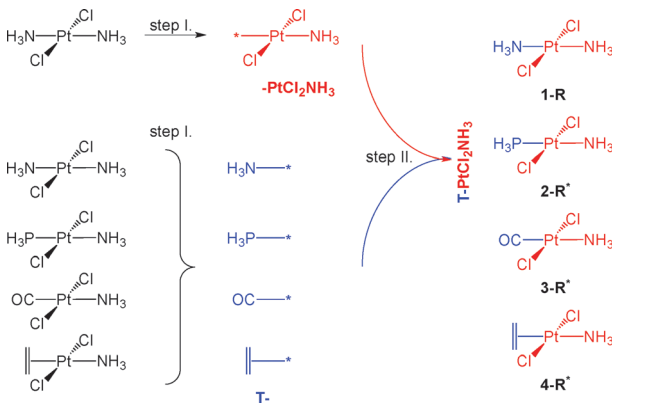

Scheme 3 Formation of model compounds **1-R**, **2-R***, **3-R*** and **4-R*** with a fixed Pt–NH_3 distance; optimized structures are used to generate the –$PtCl_2NH_3$ host fragment from $NH_3PtCl_2NH_3$ and T ligands from the corresponding $TPtCl_2NH_3$ reactants in step I. Whereas they are combined to the artificial T-$PtCl_2NH_3$ structures in step II. The following decomposition analysis is carried out between $TPtCl_2$ and NH_3 fragments.

Table 3 Pt–N1 distances in the reactant state (**R**) in Å and interaction energy (ΔE_{int}) and its components (ΔE_{Pauli}, ΔV_{elstat} and ΔE_{oi}) calculated between $TPtCl_2$ and NH_3 fragments in kcal mol^{-1}

	T	d(Pt–N1)	ΔE_{Pauli}	ΔV_{elstat}	ΔE_{oi}	ΔE_{int}
1-R	NH_3	2.059	128.2	−122.6	−60.9	−55.3
2-R	PH_3	2.119	119.8	−109.1	−52.7	−41.9
3-R	CO	2.106	126.2	−116.4	−59.3	−49.5
4-R	C_2H_4	2.114	126.0	−113.4	−55.6	−42.9

Table 4 Interaction energy (ΔE_{int}) and its components (ΔE_{Pauli}, ΔV_{elstat} and ΔE_{oi}) calculated between $TPtCl_2$ andNH_3 fragments in the constrained geometry reactants, denoted with *, with a fixed Pt–N1 distance of 2.059 Å. Values are given in kcal mol^{-1}

	T	d(Pt–N1)	ΔE_{Pauli}	ΔV_{elstat}	ΔE_{oi}	ΔE_{int}
1-R	NH_3	2.059	128.2	−122.6	−60.9	−55.3
2-R*	PH_3	2.059	142.7	−126.5	−58.0	−41.8
3-R*	CO	2.059	139.7	−128.2	−61.7	−50.3
4-R*	C_2H_4	2.059	146.9	−129.5	−60.5	−43.1

filled–filled orbital repulsion (ΔE_{Pauli}). Admittedly, electrostatics also plays a non-negligible role (3 kcal mol^{-1}) in the relative strengths of PH_3 and C_2H_4. However, the stabilizing filled–vacant orbital interaction, ΔE_{oi}, is practically unaffected by T. Hence, the Pt–N1 bond elongates when a strong T is bound to the metal to avoid an overwhelming Pauli repulsion. The reduction of the destabilizing Pauli repulsion as the ligand got further from the metal compensates for the loss in the electrostatic and stabilizing orbital interactions until the optimal Pt–N1 distance is reached.

How can the Pauli repulsion as a function of T be interpreted? To answer this question we have to note that the Pauli repulsion is calculated in the first step of the decomposition analysis, where no filled–vacant orbital mixing is allowed; it is simply the filled–filled orbital interaction in terms of the initial fragment orbitals.[39] The formed filled orbitals relax by mixing with the unoccupied orbitals of the fragments in the second step of the decomposition analysis. Before analysing which relaxed MO represents the filled–filled repulsive interaction, first the relevant molecular orbitals (MOs) of $TPtCl_2NH_3$ that represent the interactions between T, $PtCl_2$ and NH_3 (Scheme 4) moieties are introduced. For simplicity all four ligands are considered to be pure σ-donors and have the same ligand strength as well as C_s symmetry is assumed for $TPtCl_2NH_3$, thus this picture represents a first order approximation of the investigated systems.

Two filled orbitals represent the T–Pt, Pt–NH_3 and T–NH_3 interactions; 1a′ is the bonding combination of the 'lone pair' orbitals of T and NH_3 with the $d_{x^2-y^2}$ metal orbital, whereas 2a′ represents the mixing of the antibonding combination of ligand lone pairs with the p_x orbital of the metal. 3a′ and 4a′ are the corresponding antibonding combinations. Since the overlap of the lone pairs with d_{z^2} is small and both bonding and anti-bonding combinations (not shown) are filled, the contribution of these interactions to the metal–ligand bonding is negligible.

Most importantly, there is no relaxed occupied molecular orbital, in first order approximation, that would represent the repulsive interaction *between the metal and ligand NH_3*. Rather, it turns out that the critical feature is the antibonding relationship of the two ligands *trans* to each other, T and NH_3, which is transferred by the p_x molecular orbital. Thus, the relaxed molecular orbital that can be associated with the affected Pauli repulsion is 2a′. The latter orbital represents attraction (bonding type interaction) between the metal and T as well as between the metal and NH_3, but repulsion (antibonding type interaction) between T and NH_3. Accordingly, 2a′ embodies all the requirements to be expected from a molecular orbital conducting the *trans* influence; directionality, namely that *cis* ligands have no direct effect on it, and the competitive relation of the ligands *trans* to each other.

The latter analysis clearly reveals the pivotal role of ligand T in determining the stability of the reactant state and also provided a straightforward rationalization for it. For the complete understanding of the *trans* effect, however, we also have to explain how T stabilizes/destabilizes the transition state. As it was shown above (Table 2) the interaction energy calculated between fragments $TPtCl_2$ and $(NH_3)_2$ in the transition states only allow the differentiation of ligands with and without π-acid property. Decomposition of this interaction energy reveals simple trends, but, then again, is affected strongly by the distance dependency of the energy components; Pauli repulsion is stronger, whereas orbital and electrostatic interactions are more attractive for a more compact transition state (Table 2). To eliminate the effect of this distance dependency of the various energy components when comparing the transition states of the four investigated systems, we applied again the procedure that was introduced above for the reactant state. Now, the $PtCl_2(NH_3)_2$ part of the structure is fixed to the geometry of $NH_3PtCl_2(NH_3)_2$ and it will be augmented with the *trans* ligands T using the geometry what they adopt in their corresponding transition states. The energy decomposition analysis is now carried out between the $TPtCl_2$ and $(NH_3)_2$ fragments.

The interaction energies calculated for the constrained transition state structures are very similar (within 1 kcal mol^{-1}) to that of the equilibrium TS structure (Table 2 *vs.* Table 5) indicating that the induced error by this method is again negligible. Since the various components of the interaction energy and accordingly the total interaction energy are very similar for pure σ-donors, this type of analysis indicates that the σ-donation ability has no specific stabilization/destabilization contribution in the TS. In contrast, π-acids influence the stability of the transition state; CO enhances the stabilizing interactions (orbital and electrostatic) whereas C_2H_4 reduces the filled–filled orbital repulsion.

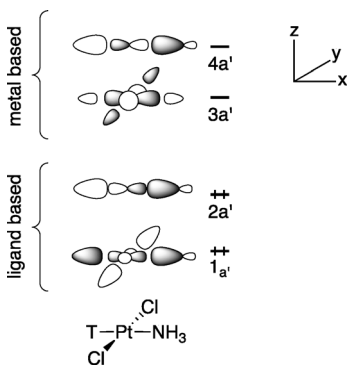

Scheme 4 Molecular orbitals representing the bonding interactions (1a′ and 2a′) between T, Pt and NH_3 given with the corresponding antibonding combinations (3a′ and 4a′).

Table 5 Interaction energy (ΔE_{int}) and its components (ΔE_{Pauli}, ΔV_{elstat} and ΔE_{oi}) calculated between $TPtCl_2$ and $(NH_3)_2$ fragments at fixed Pt–N1 and Pt–N2 distances (d(Pt–N)) of 2.448 Å. Values are given in kcal mol^{-1}. * denotes that these are structures with a constrained geometry (see text)

	T	d(Pt–N)	ΔE_{Pauli}	ΔV_{elstat}	ΔE_{oi}	ΔE_{int}
1-TS	NH_3	2.448	89.1	−83.9	−43.9	−38.6
2-TS*	PH_3	2.448	89.5	−83.8	−45.1	−39.4
3-TS*	CO	2.448	89.4	−88.3	−50.3	−49.2
4-INT*	C_2H_4	2.448	82.2	−83.4	−46.8	−48.0

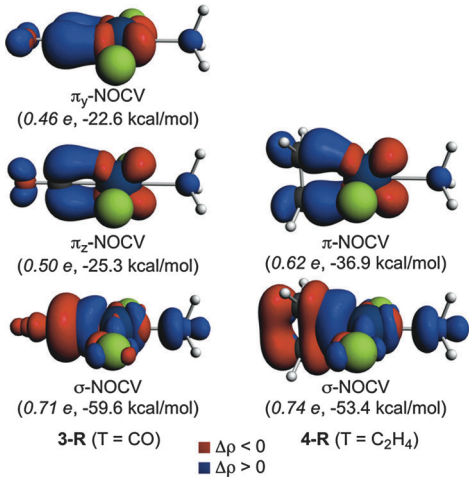

Fig. 4 NOCV orbitals representing the σ-donation from CO and C_2H_4 to the metal and π-backdonation from the metal to the π* orbitals of CO and C_2H_4 in **3-R** and **4-R**, respectively.

Applying NOCV orbitals we will consequently gain insight into the different behaviour of CO and C_2H_4 in stabilizing the TS. Conceptually two types of backdonation can be distinguished; the *intrinsic* one is already present in the reactant state whereas the surplus backdonation generated by the incoming–outgoing ligands in the TS is called *induced* backdonation. Our hypothesis is that for CO and C_2H_4 the magnitude of intrinsic/induced π-backdonations is different which is manifested in different components of the interaction energy.

Fig. 4 and 5 show the relevant NOCVs along the T–Pt interaction for CO and C_2H_4 in the square planar reactant and trigonal bipyramid structure, respectively. The σ-donation and the π-backdonations to the π* orbitals of CO of C_2H_4 can be easily recognized on these intuitively appearing orbitals. The amount of electrons transferred and the associated stabilization energy are also indicated in these figures, which indeed shows that both intrinsic and induced backdonations differ in the two systems. Already in the reactant state C_2H_4 reduces the density in the plane of incoming–outgoing ligands (the *xz* plane) more effectively (0.62e) than CO (0.50e). Going from the reactant to the transition state the magnitude of induced backdonation is similar, about 0.1e, however, it causes significantly larger stabilization in CO than in C_2H_4. In addition, backdonation to two π* orbitals in CO actually makes the metal more positive compared to C_2H_4 which can be seen in the better electrostatic interaction in the former.

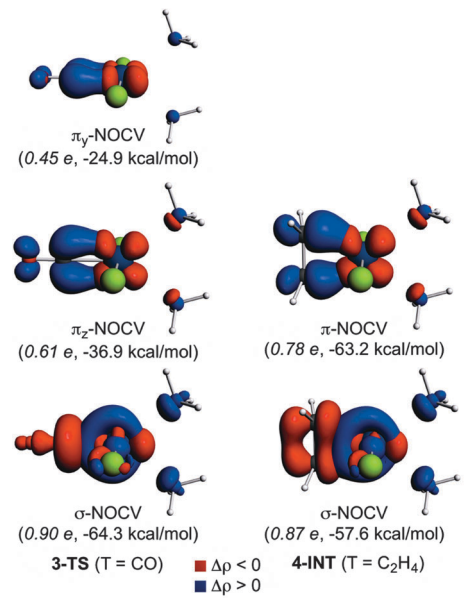

Fig. 5 NOCV orbitals representing the σ-donation from CO and C_2H_4 to the metal and π-backdonation from the metal to the π* orbitals of CO and C_2H_4 in **3-TS** and **4-INT**, respectively.

Discussions

In the analysis above it was quantitatively shown that the σ-donor ability of the *trans* ligand (T) indeed controls the stability of the reactant whereas π-backdonation to T stabilizes the transition state. For the former, we clearly demonstrated that the reactant is destabilized and the ligand *trans* to T is labilized due to the repulsion of ligand T exerted on the ligand *trans* to itself. It is however not in line with the widely accepted interpretation that ligands *trans* to each other compete for donation ability, and if one donates more electrons to the metal, the other loses its ability to donate and consequently its bond to the metal becomes weaker. Since these two hypotheses are conceptually quite dissimilar from each other we critically discuss how they contradict or complement each other. To do so, first we interpret the σ-*trans* effect and *trans* influence strength of ligands in terms of electron density and also within the molecular orbital framework using repulsion-based arguments.

The *trans* influence and the σ-*trans* effect can be interpreted in terms of electron density as follows. In the formation of a ligand to metal dative bond, the donated electron density is not only accumulated between the metal and the ligand, but also on the coordination site *trans* to the ligand. Due to this density accumulation in the *trans* position, a ligand in this position will be exposed to a Pauli-type repulsion, besides the attraction from the positive metal centre. Thus, increasing σ-donation results in a stronger repulsion in the *trans* position, which induces the elongation and labilization of the metal–ligand bond.

This is in line with the findings of Lin and Hall,[10] who demonstrated the repulsion between lone-pairs of the incoming/leaving ligands and the central metal using the Laplacian of the electron density. In this study, the preferred positions and orientations of the reacting ligands were rationalized with the minimization of this repulsion in the course of the reaction. The *trans* effect also was interpreted as the effect of the *trans* ligand on this repulsion *in the transition state.*[10] Our analysis readjusts Hall's hypothesis, however, for the σ-subspace: the repulsion has to be maximized in the reactant by σ-donation to labilize the leaving group and destabilize the reactant. In the π-subspace we indeed found that the intrinsic π-backdonation

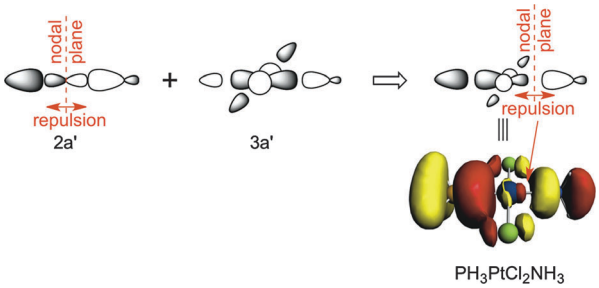

Scheme 5 Increasing repulsion in terms of hybridization of 2a′ with 3a′.

reduces the repulsion between the reacting ligands and the metal containing fragment in the transition state.

How can the σ-*trans* effect strength of ligands be interpreted within the molecular orbital framework? In this study we deduce that it has to be the metal p_x orbital that transfers the repulsion between ligands *trans* to each other, however, we did not address the question how a weaker or a stronger repulsion is manifested in the molecular orbitals. An MO concept that is consistent with the proposed repulsion-based argument was actually given by Burdett and Albright in the same study,[9f] in which they introduced the concept of orbital sharing discussed in the Introduction (*e.g.* eqn (1a) and (1b)). According to this MO picture, when T differs from the leaving group the reduced symmetry of the molecule allows the mixing of the 2a′ orbital with the metal-based virtual 3a′ orbital as shown in Scheme 5. Such a hybridization results in the strengthening of the metal–ligand interaction on the side of the stronger donor and weakening of the bond *trans* to it; Scheme 5 clearly shows the shift of the nodal plane towards the weaker donor ligand. With increasing donor strength of T, *i.e.* as T gets less electronegative, the hybridization is enhanced and more and more repulsive interaction is introduced *trans* to T in line with our quantitative analysis.

Both the density- and the MO-based arguments can thus be translated into an even simpler chemical concept, namely the repulsion exerted by T can be seen as the donation from T to the σ* orbital of the metal-leaving group bond. σ-NOCV orbitals in Fig. 4 unambiguously demonstrate that in forming the T–Pt bond the density is not only accumulated between T and Pt, but also between Pt and NH_3 (the leaving group) in an antibonding fashion: the presence of the nodal plane can be easily recognized between Pt and NH_3 in Fig. 4, which evidences the repulsion between these fragments as T binds to the metal.

It is very important to recognize that the repulsion of groups *trans* to each other does not exclude contributions from orbital sharing – the effect of competition for donation – in weakening the metal-leaving group bond. We propose that both effects operate simultaneously in these systems as it was also proposed by Albright and Burdett: ''In other cases, notably the *trans* influence, both effects (orbital sharing and hybridization) may be important''.[9f] Our quantitative analysis, however, revealed that the effect of repulsion is more dominant than that of the limitation of donation. For example, PH_3, besides that it exerts a Pauli repulsion of 14.5 kcal mol^{-1} stronger than NH_3 (Table 4), it also makes the orbital interaction *trans* to it less attractive by about 3 kcal mol^{-1} compared to NH_3, which can be indeed attributed to the limited donation of the leaving group.

Conclusions

The mechanisms with which *trans* ligands (T) can manipulate the activation barriers of ligand substitutions *trans* to themselves were investigated. It was evidenced quantitatively that the σ-donor ability of T indeed controls the stability of the reactant, whereas in the case of π-acids, backdonation stabilizes the transition state, for which conceptually two mechanisms are available: intrinsic and induced π-backdonation. The former, which operates already in the reactant state results in a smaller repulsion between electrons of the metal and the lone-pairs of the incoming/outgoing ligands. The excess backdonation induced by the presence of both incoming and outgoing ligands in the TS further stabilizes the TS over the reactant. We found that the σ-donation ability has a negligible effect on the stabilization/destabilization of the transition state.

Our most important conclusion is that competition for donation or, in other words the limitation of donation by the *trans* ligand, is of minor importance in the destabilization of the reactant and also in the labilization of the leaving group. Rather, Pauli repulsion causes the weakening of the metal–ligand bond *trans* to a good σ-donor ligand. We have shown that the donated density is not only accumulated between the metal and the donor ligand but also on the *trans* site of the metal and, thus, a ligand in this position is not only subject to the attraction of the metal, but also to the repulsion of this electron cloud. In molecular orbital terminology this is a filled–filled orbital repulsion between the two ligands *trans* to each other, represented by the antibonding combination of the lone pairs of these ligands, conducted, in first order, by the metal p_x orbital. With increasing σ-donation strength of the *trans* ligand the latter orbital mixes more and more into the $d_{x^2-y^2}$-based vacant orbital (Scheme 5), which results in a more repulsive metal–ligand interaction in the *trans* position. The latter process can also be envisioned as the donation from the *trans* ligand to the σ* orbital of the metal–ligand bond *trans* to it, which was clearly demonstrated by the σ-type NOCV orbitals, *i.e.* the deformation density upon bond formation (Fig. 4). Thus, both the σ-*trans* effect (destabilization of the reactant) and the *trans* influence (elongation of the metal–ligand bond in the reactant) were originated from the repulsion between the $TPtCl_2$ and NH_3 fragments, induced by the *trans* ligand T.

It is known for a while that the mechanism of ligand substitution of square planar complexes can deviate from the representative interchange mechanism depending on the *trans* ligand, for example, strong donor *trans* ligands without π-acid property, such as H^- and CH_3^-, tend to prefer a dissociative interchange mechanism. Moreover, even for weaker donors a continuous spectrum of mechanisms with equally probable interchange and dissociative pathways was recently proposed based on *ab initio* molecular metadynamic simulations.[40]

We believe that the proposed repulsion-based rationalization is more consistent with this observation than orbital sharing-based ones because even in the case of an extreme orbital sharing effect, where the *trans* ligand completely blocks the binding of the leaving group to the corresponding d orbital, $d_{x^2-y^2}$, the metal p orbital would be still available for the leaving group to form a bond with the metal. Stable d^{10} complexes evidence that such bonds are not necessarily weak at all and, thus, the spontaneous loss of the leaving group in the dissociative pathway rather occurs due to the repulsion of the *trans* ligand. In addition, the push-out of the leaving group concept is the only way to explain the controversial behaviour that electron donation actually increases the nucleophilic reactivity of these systems.

We also demonstrated that energy decomposition analysis on constrained structures, with or without coupling to the energy decomposition along the reaction path and/or NOCV analysis, is a powerful tool in understanding complicated chemical processes and phenomena. If the artificial error induced with the constraint is small, similarly to the investigated systems, this method can be used with confidence and novel insights into the origins and underlying principles of various phenomena can be gained, which might be otherwise hidden by the distance dependence of the electrostatic, orbital and Pauli interactions.

Acknowledgements

P.G and F.D.P. wish to acknowledge the Research Foundation-Flanders (FWO) and the Free University of Brussels (VUB) for continuous support to the ALGC research group. The authors also wish to acknowledge the financial support from a Research Program of the Research Foundation – Flanders (FWO) (G.0119.09N). B.P. would like to thank OTKA (HUMAN_MB08-1-2011-0018) for financial support.

Notes and references

1 (*a*) C. H. Langford and H. B. Gray, *Ligand Substitution Processes*, W. A. Benjamin, Inc., New York, 1966; (*b*) F. Basolo, *Mechanisms of Inorganic Reactions*, American Chemical Society, 1965, p. 280; (*c*) J. D. Atwood, *Inorganic and Organometallic Reaction Mechanisms*, John Wiley & Sons, Canada, 1985; (*d*) M. L. Tobe, J. Burgess and A. Wesley, *Inorganic Reaction Mechanisms*, Longman Inc., 1999.

2 (*a*) B. J. Coe and S. J. Glenwright, *Coord. Chem. Rev.*, 2000, **203**, 5; (*b*) E. M. Shustorovich, M. A. Porai-Koshits and Y. A. Buslaev, *Coord. Chem. Rev.*, 1975, **17**, 1.

3 (*a*) M.-H. Baik, R. A. Friesner and S. J. Lippard, *J. Am. Chem. Soc.*, 2003, **125**, 14082; (*b*) H. S. Noel, S. Jens and B. George, *Coord. Chem. Rev.*, 2005, **249**, 299; (*c*) J. Raber, C. Zhu and L. A. Eriksson, *J. Phys. Chem. B*, 2005, **109**, 11006; (*d*) Z. Yong, G. Zijian and Y. Xiao-Zeng, *J. Am. Chem. Soc.*, 2001, **123**, 9378; (*e*) J. V. Burda, M. Zeizinger and J. Leszczynski, *J. Comput. Chem.*, 2005, **26**, 907; (*f*) L. A. S. Costa, T. W. Hambley, W. R. Rocha, W. B. De Almeida and H. F. Dos Santos, *Int. J. Quantum Chem.*, 2006, **106**, 2129; (*g*) L. A. S. Costa, W. R. Rocha, W. B. De Almeida and H. F. Dos Santos, *J. Chem. Phys.*, 2003, **118**, 10584; (*h*) A. Dedieu, *Chem. Rev.*, 2000, **100**, 543; (*i*) D. V. Deubel, *J. Am. Chem. Soc.*, 2006, **128**, 1654; (*j*) M. A. Fuertes, C. Alonso and J. M. Pérez, *Chem. Rev.*, 2003, **103**, 645; (*k*) E. R. Jamieson and S. J. Lippard, *Chem. Rev.*, 1999, **99**, 2467; (*l*) J. K.-C. Lau and D. V. Deubel, *J. Chem. Theory Comput.*, 2005, **2**, 103; (*m*) M. Milan and C. E. Holloway, *Coord. Chem. Rev.*, 2006, **250**, 2261; (*n*) E. Wong and C. M. Giandomenico, *Chem. Rev.*, 1999, **99**, 2451; (*o*) Y. Mantri, S. J. Lippard and M.-H. Baik, *J. Am. Chem. Soc.*, 2007, **129**, 5023; (*p*) C. Zdenek and Š. Miroslav, *Collect. Czech. Chem. Commun.*, 2003, **68**, 1105.

4 (*a*) R. Álvarez, O. N. Faza, C. S. López and Á. R. de Lera, *Org. Lett.*, 2005, **8**, 35; (*b*) A. Ariafard, Z. Lin and I. J. S. Fairlamb, *Organometallics*, 2006, **25**, 5788; (*c*) A. A. C. Braga, N. H. Morgon, G. Ujaque and F. Maseras, *J. Am. Chem. Soc.*, 2005, **127**, 9298; (*d*) A. A. C. Braga, G. Ujaque and F. Maseras, *Organometallics*, 2006, **25**, 3647; (*e*) E. R. Davidson, *Chem. Rev.*, 2000, **100**, 351; (*f*) D. García-Cuadrado, A. A. C. Braga, F. Maseras and A. M. Echavarren, *J. Am. Chem. Soc.*, 2006, **128**, 1066; (*g*) D. García-Cuadrado, P. de Mendoza, A. A. C. Braga, F. Maseras and A. M. Echavarren, *J. Am. Chem. Soc.*, 2007, **129**, 6880; (*h*) L. J. Goossen, D. Koley, H. L. Hermann and W. Thiel, *J. Am. Chem. Soc.*, 2005, **127**, 11102; (*i*) L. J. Goossen, D. Koley, H. L. Hermann and W. Thiel, *Organometallics*, 2005, **25**, 54; (*j*) Y.-L. Huang, C.-M. Weng and F.-E. Hong, *Chem.–Eur. J.*, 2008, **14**, 4426; (*k*) S. Kozuch, C. Amatore, A. Jutand and S. Shaik, *Organometallics*, 2005, **24**, 2319; (*l*) E. Napolitano, V. Farina and M. Persico, *Organometallics*, 2003, **22**, 4030; (*m*) A. Nova, G. Ujaque, F. Maseras, A. Lledós and P. Espinet, *J. Am. Chem. Soc.*, 2006, **128**, 14571; (*n*) T. Ziegler, *Chem. Rev.*, 1991, **91**, 651; (*o*) A. A. C. Braga, N. H. Morgon, G. Ujaque, A. Lledós and F. Maseras, *J. Organomet. Chem.*, 2006, **691**, 4459; (*p*) M. Sumimoto, N. Iwane, T. Takahama and S. Sakaki, *J. Am. Chem. Soc.*, 2004, **126**, 10457.

5 (*a*) J. Kua, X. Xu, R. A. Periana and W. A. Goddard, *Organometallics*, 2001, **21**, 511; (*b*) M. Lersch and M. Tilset, *Chem. Rev.*, 2005, **105**, 2471; (*c*) K. Mylvaganam, G. B. Bacskay and N. S. Hush, *J. Am. Chem. Soc.*, 2000, **122**, 2041; (*d*) A. Paul and C. B. Musgrave, *Organometallics*, 2007, **26**, 793; (*e*) P. E. M. Siegbahn, *J. Phys. Chem.*, 1995, **99**, 12723; (*f*) S. S. Stahl, J. A. Labinger and J. E. Bercaw, *Angew. Chem., Int. Ed.*, 1998, **37**, 2180; (*g*) X. Xu, J. Kua, R. A. Periana and W. A. Goddard, *Organometallics*, 2003, **22**, 2057; (*h*) H. Zhu and T. Ziegler, *J. Organomet. Chem.*, 2006, **691**, 4486; (*i*) H. Zhu and T. Ziegler, *Organometallics*, 2007, **26**, 2277; (*j*) H. Zhu and T. Ziegler, *Organometallics*, 2008, **27**, 1743; (*k*) H. Zhu and T. Ziegler, *Organometallics*, 2009, **28**, 2773.

6 (*a*) F. Basolo, H. B. Gray and R. G. Pearson, *J. Am. Chem. Soc.*, 1960, **82**, 4200; (*b*) U. Belluco, L. Cattalini and A. Turco, *J. Am. Chem. Soc.*, 1964, **86**, 226; (*c*) U. Belluco, L. Cattalini and A. Turco, *J. Am. Chem. Soc.*, 1964, **86**, 3257;

(*d*) O. F. Wendt and L. I. Elding, *J. Chem. Soc., Dalton Trans.*, 1997, 4725; (*e*) R. Gosling and M. L. Tobe, *Inorg. Chem.*, 1983, **22**, 1235; (*f*) N. Kuznik and O. F. Wendt, *J. Chem. Soc., Dalton Trans.*, 2002, 3074; (*g*) S. Otto and L. I. Elding, *J. Chem. Soc., Dalton Trans.*, 2002, 2354; (*h*) O. F. Wendt and L. I. Elding, *Inorg. Chem.*, 1997, **36**, 6028; (*i*) B. Umberto, C. Lucio and T. Aldo, *J. Am. Chem. Soc.*, 1964, **86**, 226.

7 L. G. Vanquickenborne, J. Vranckx and C. Goeller-Walrand, *J. Am. Chem. Soc.*, 1974, **96**, 4121.

8 S. S. Zumdahl and R. S. Drago, *J. Am. Chem. Soc.*, 1968, **90**, 6669.

9 (*a*) J. Chatt, L. A. Duncanson and L. M. Venanzi, *J. Chem. Soc.*, 1955, 4456; (*b*) M. Randic, *J. Chem. Phys.*, 1962, **36**, 3278; (*c*) L. E. Orgel, *J. Inorg. Nucl. Chem.*, 1956, **2**, 137; (*d*) A. A. Grinberg, *Acta Physicochim. URSS*, 1935, **3**, 573; (*e*) M. P. Mitoraj, H. Zhu, A. Michalak and T. Ziegler, *Int. J. Quantum Chem.*, 2009, **109**, 3379; (*f*) J. K. Burdett and T. A. Albright, *Inorg. Chem.*, 1979, **18**, 2112.

10 Z. Lin and M. B. Hall, *Inorg. Chem.*, 1991, **30**, 646.

11 Z. Chval, M. Sip and J. V. Burda, *J. Comput. Chem.*, 2008, **29**, 2370.

12 J. K.-C. Lau and D. V. Deubel, *Chem.–Eur. J.*, 2005, **11**, 2849.

13 T. G. Appleton, H. C. Clark and L. E. Manzer, *Coord. Chem. Rev.*, 1973, **10**, 335.

14 N. N. Greenwood and A. Earnshaw, *Chemistry of the Elements*, Butterworth Heinemann, Oxford, 1997.

15 K. M. Anderson and A. G. Orpen, *Chem. Commun.*, 2001, 2682.

16 C. E. Housecroft and A. G. Sharpe, *Inorganic Chemistry*, Prentice Hall, Harlow, 2001.

17 (*a*) P. K. Sajith and C. H. Suresh, *Dalton Trans.*, 2010, **39**, 815; (*b*) P. K. Sajith and C. H. Suresh, *J. Organomet. Chem.*, 2011, **696**, 2086.

18 (*a*) J. Zhu, Z. Lin and T. B. Marder, *Inorg. Chem.*, 2005, **44**, 9384; (*b*) P. N. Kapoor and R. Kakkar, *J. Mol. Struct.*, 2004, **679**, 149.

19 (*a*) Backdonation can occur to the σ^* orbital of PH_3, however, it is of minor importance compared to CO and C_2H_4; (*b*) P. D. Lyne and D. M. P. Mingos, *J. Organomet. Chem.*, 1994, **478**, 141; (*c*) D. S. Marynick, *J. Am. Chem. Soc.*, 1984, **106**, 4064.

20 Y. Zhao and D. Truhlar, *Theor. Chem. Acc.*, 2008, **120**, 215.

21 (*a*) D. Figgen, G. Rauhut, M. Dolg and H. Stoll, *Chem. Phys.*, 2005, **311**, 227; (*b*) K. A. Peterson and C. Puzzarini, *Theor. Chim. Acta*, 2005, **114**, 283.

22 (*a*) D. E. Woon and J. T. H. Dunning, *J. Chem. Phys.*, 1993, **98**, 1358; (*b*) T. H. Dunning, *J. Chem. Phys.*, 1989, **90**, 1007.

23 (*a*) R. A. Kendall, T. H. Dunning and R. J. Harrison, *J. Chem. Phys.*, 1992, **96**, 6796; (*b*) D. Figgen, K. A. Peterson, M. Dolg and H. Stoll, *J. Chem. Phys.*, 2009, **130**, 164108.

24 M. J. Frisch, G. W. Trucks, H. B. Schlegel, G. E. Scuseria, M. A. Robb, J. R. Cheeseman, G. Scalmani, V. Barone, B. Mennucci, G. A. Petersson, H. Nakatsuji, M. Caricato, X. Li, H. P. Hratchian, A. F. Izmaylov, J. Bloino, G. Zheng, J. L. Sonnenberg, M. Hada, M. Ehara, K. Toyota, R. Fukuda, J. Hasegawa, M. Ishida, T. Nakajima, Y. Honda, O. Kitao, H. Nakai, T. Vreven, J. A. Montgomery, J. E. Peralta, F. Ogliaro, M. Bearpark, J. J. Heyd, E. Brothers, K. N. Kudin, V. N. Staroverov, R. Kobayashi, J. Normand, K. Raghavachari, A. Rendell, J. C. Burant, S. S. Iyengar, J. Tomasi, M. Cossi, N. Rega, J. M. Millam, M. Klene, J. E. Knox, J. B. Cross, V. Bakken, C. Adamo, J. Jaramillo, R. Gomperts, R. E. Stratmann, O. Yazyev, A. J. Austin, R. Cammi, C. Pomelli, J. W. Ochterski, R. L. Martin, K. Morokuma, V. G. Zakrzewski, G. A. Voth, P. Salvador, J. J. Dannenberg, S. Dapprich, A. D. Daniels, J. Farkas, B. Foresman, J. V. Ortiz, J. Cioslowski and D. J. Fox, *Gaussian 09, Revision B.01*, Wallingford, CT, 2009.

25 (*a*) R. J. Bartlett, *J. Phys. Chem.*, 1989, **93**, 1697; (*b*) G. D. Purvis and R. J. Bartlett, *J. Phys. Chem.*, 1982, **76**, 1919; (*c*) K. Raghavachari, G. W. Trucks, M. Head-Gordon and J. A. Pople, *Chem. Phys. Lett.*, 1989, **157**, 479; (*d*) G. E. Scuseria, C. L. Janssen and H. F. Schaefer III, *J. Chem. Phys.*, 1988, **89**, 7382.

26 (*a*) H.-J. Werner, P. J. Knowles, G. Knizia, F. R. Manby and M. Schütz, *Wiley Interdiscip. Rev.: Comput. Mol. Sci.*, 2012, **2**, 242; (*b*) H.-J. Werner, P. J. Knowles, G. Knizia, F. R. Manby and M. Schütz, *et al.*, *Wiley Interdiscip. Rev.: Comput. Mol. Sci.*, 2012, **2**, 242.

27 (*a*) J. P. Perdew, K. Burke and M. Ernzerhof, *Phys. Rev. Lett.*, 1996, **77**, 3865; (*b*) J. P. Perdew, K. Burke and M. Ernzerhof, *Phys. Rev. Lett.*, 1997, **78**, 1396.

28 (*a*) G. te Velde, F. M. Bickelhaupt, E. J. Baerends, C. F. Guerra, S. J. A. van Gisbergen, J. G. Snijders and T. Ziegler, *J. Comput. Chem.*, 2001, **22**, 931; (*b*) E. v. Lenthe, E. J. Baerends and J. G. Snijders, *J. Chem. Phys.*, 1993, **99**, 4597; (*c*) E. van Lenthe, R. van Leeuwen, E. J. Baerends and J. G. Snijders, *Int. J. Quantum Chem.*, 1996, **57**, 281.

29 E. J. Baerends, J. Autschbach, D. Bashford, A. Børces, F. M. Bickelhaupt, C. Bo, P. M. Boerrigter, L. Cavallo, D. P. Chong, L. Deng, R. M. Dickson, D. E. Ellis, M. van Faassen, M. Fan, T. H. Fischer, C. F. Guerra, A. Ghysels, A. Giammona, S. J. A. van Gisbergen, A. W. Gotz, J. A. Groeneveld, O. V. Gritsenko, M. Grüning, F. E. Harris, P. Harris, P. van den Hoek, C. R. Jacob, H. Jacobsen, L. Jensen, G. van Kessel, F. Kootstra, M. V. Krykunov, E. van Lenthe, D. A. McCormack, A. Michalak, M. Mitoraj, J. Neugebauer, V. P. Nicu, L. Noodleman, V. P. O. Osinga, S. Patchkovskii, P. H. T. Philipsen, D. Post, C. C. Pye, W. Ravenek, J. I. Rodriguez, P. Ros, P. R. T. Schipper, G. Schreckenbach, M. Seth, J. G. Snijders, M. Solà, M. Swart, D. Swerhone, G. te Velde, P. Vernooijs, L. Versluis, L. Visscher, O. Visser, F. Wang, T. A. Wesolowski, E. M. van Wezenbeek, G. Wiesenekker, S. K. Wolff, T. K. Woo, A. L. Yakovlev and T. Ziegler, *ADF2010.02*, V. U, Amsterdam, The Netherlands, 2009.

30 (*a*) W.-J. van Zeist and F. M. Bickelhaupt, *Org. Biomol. Chem.*, 2010, **8**, 3118; (*b*) F. M. Bickelhaupt, *J. Comput. Chem.*, 1999, **20**, 114.

31 (*a*) F. M. Bickelhaupt and E. J. Baerends, *Rev. Comput. Chem.*, 2000, **15**, 1; (*b*) T. Ziegler and A. Rauk, *Theor. Chim. Acta*, 1977, **46**, 1; (*c*) T. Ziegler and A. Rauk, *Inorg. Chem.*,

1979, **18**, 1558; (*d*) T. Ziegler and A. Rauk, *Inorg. Chem.*, 1979, **18**, 1755.

32 B. Pinter, T. Fievez, F. M. Bickelhaupt, P. Geerlings and F. De Proft, *Phys. Chem. Chem. Phys.*, 2012, **14**, 9846.

33 (*a*) M. Mitoraj and A. Michalak, *J. Mol. Model.*, 2007, **13**, 347; (*b*) M. P. Mitoraj, A. Michalak and T. Ziegler, *J. Chem. Theory Comput.*, 2009, **5**, 962; (*c*) M. P. Mitoraj, M. Parafiniuk, M. Srebro, M. Handzlik, A. Buczek and A. Michalak, *J. Mol. Model.*, 2011, **17**, 2337.

34 (*a*) A. P. Bento and F. M. Bickelhaupt, *J. Org. Chem.*, 2007, **72**, 2201; (*b*) M. A. van Bochove, M. Swart and F. M. Bickelhaupt, *J. Am. Chem. Soc.*, 2006, **128**, 10738; (*c*) S. C. A. H. Pierrefixe, C. F. Guerra and F. M. Bickelhaupt, *Chem.–Eur. J.*, 2008, **14**, 819; (*d*) W.-J. van Zeist and F. M. Bickelhaupt, *Chem.–Eur. J.*, 2010, **16**, 5538.

35 (*a*) I. Fernández, G. Frenking and E. Uggerud, *Chem.–Eur. J.*, 2009, **15**, 2166; (*b*) I. Fernández, G. Frenking and E. Uggerud, *J. Org. Chem.*, 2010, **75**, 2971.

36 A negative critical energy does not mean that the process is barrierless; taking into consideration solvent effects and thermodynamic corrections, especially translational entropy, activation energies become positive, as expected. Nevertheless, our analysis suggests (Table S1, ESI†) that the choice of reference does not affect the conclusions in the investigated processes.

37 J. Cooper and T. Ziegler, *Inorg. Chem.*, 2002, **41**, 6614.

38 As Table 1 shows the inclusion of thermal corrections into the activation energy does not change the relative order of the barriers, and it is relatively uniform along the investigated series. Since the overall charge of the systems does not change during the reaction, a similar solvent effect can also be expected for these systems. It should be noted, however, that these effects can make quite a difference in other systems, even though they might cancel each other sometimes as shown in ref. 37.

39 F. M. Bickelhaupt and E. J. Baerends, *Kohn–Sham Density Functional Theory: Predicting and Understanding Chemistry*, John Wiley & Sons, Inc., 2007.

40 J. K.-C. Lau and B. Ensing, *Phys. Chem. Chem. Phys.*, 2010, **12**, 10348.